# Topologic Attention Networks: Attending to Direct and Indirect Neighbors through Gaussian Belief Propagation

## Marshall Rosenhoover

Department of Computer Science University of Alabama in Huntsville marshall.rosenhoover@uah.edu

## **Huaming Zhang**

Department of Computer Science University of Alabama in Huntsville huaming.zhang@uah.edu

# **Abstract**

Graph Neural Networks rely on local message passing, which limits their ability to model long-range dependencies in graphs. Existing approaches extend this range through continuous-time dynamics or dense self-attention, but both suffer from high computational cost and limited scalability. We propose Topologic Attention Networks, a new framework that applies topologic attention, a probabilistic mechanism that learns how information should flow through both direct and indirect connections in a graph. Unlike conventional attention that depends on explicit pairwise interactions, topologic attention emerges from the learned information propagation of the graph, enabling unified reasoning over local and global relationships. This method achieves provides state-of-the-art performance across all measured baseline models. Our implementation is available at https://github.com/Marshall-Rosenhoover/Topologic-Attention-Networks.

## 1 Introduction

An intrinsic component of Graph Neural Networks (GNNs) is neighborhood aggregation: combining information from a node's neighbors to compute its representation. Many standard GNNs, such as graph convolutional networks [1] and graph attention networks [2], rely on aggregation functions that are only determined by immediate neighbors. This local aggregation limits expressiveness and can struggle to capture long-range dependencies [3, 4]. Determined to solve this problem, two main branches have emerged to aggregate information beyond the local neighborhood: continuous dynamic GNNs and graph transformers.

Continuous dynamic GNNs, such as Graph Neural ODE [5] and Continuous Graph Neural Networks [6], extend message passing into continuous time by parameterizing information flow as a differential equation or continuous-time dynamical system. This formulation allows, in principle, unbounded propagation depth and smooth global interactions. However, these methods are prone to vanishing or exploding gradients, and remain inherently sequential [5–7].

Graph transformers [8, 9] take the opposite approach by applying self-attention over a range of node representations to capture relationships beyond immediate neighbors. By encoding structural priors into node embeddings, they can capture complex relational patterns without explicit message passing. Yet, this expressivity comes at high compute and memory costs, and the effective incorporation of graph structure remains a nontrivial challenge [10].

In this work, we propose a third branch of dynamic neighborhood aggregation: Topologic Attention Networks (TANs). Unlike continuous dynamic GNNs, which require sequential integration, or graph transformers, which depend on dense pairwise attention, TANs perform topologic attention, learning how information should flow probabilistically through the graph's topology to capture both local

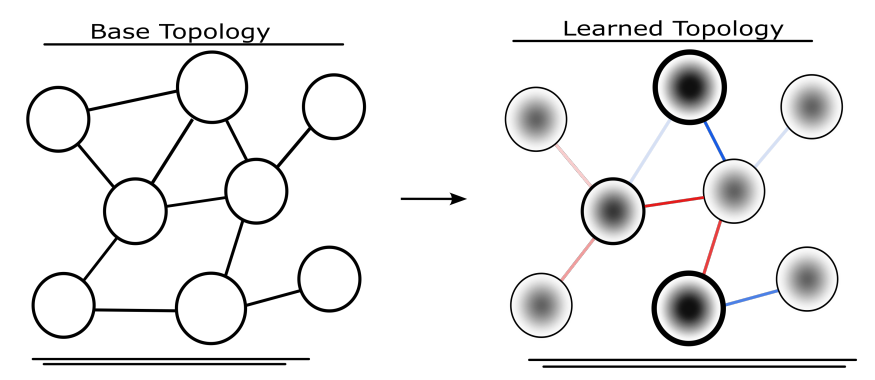


Figure 1: Illustration of a single head of topologic attention via a learned Gaussian Graphical Model, where node shading encodes confidence and edge color denotes interaction polarity and strength.

and global relationships. Figure 1 illustrates a potential learned topologic attention pattern. Laying the foundation for this new branch, we present the Topologic Attention Layer, a GNN layer that implements topologic attention. We evaluate our method across diverse graph benchmarks and find that they achieve accuracy comparable to or exceeding state-of-the-art methods, highlighting the potential of topologic attention for local and global reasoning in graphs.

# 2 Background

A linear transformation on a graph (graph linear transformation) can be understood as a global operator that mixes node features according to the connectivity of the graph. Achieving this would require each node to integrate information from all other nodes along every possible path that connects them. However, capturing these higher-order dependencies explicitly is intractable, as enumerating all such paths is known to be NP-hard [11, 12]. Instead of constructing this transformation explicitly, we can reinterpret the graph as a Gaussian graphical model whose equilibrium yields the solution to the graph linear transformation. In this formulation, Gaussian dependencies implicitly accumulate the influence of all paths in the graph, eliminating the need to enumerate them.

## 2.1 Gaussian Graphical Models

Gaussian Graphical Models represent a set of continuous random variables  $x = [x_1, \dots, x_N]^{\top}$  that follow a joint multivariate Gaussian distribution with covariance matrix  $\Sigma$ . Each variable is associated with a node in a graph, where edges capture conditional dependencies between variables. The precision matrix  $J = \Sigma^{-1}$  encodes these conditional dependencies with nonzero entries  $J_{ij}$  indicate edges between nodes [13–15]. Together with this structural information, the model includes an information vector h representing the nodes' local evidence. The pair (J,h) fully defines the probabilistic state of the system, with the joint distribution

$$p(x) \propto \exp\left(-\frac{1}{2}x^{\top}Jx + h^{\top}x\right),$$

where  $J \in \mathbb{R}^{N \times N}$ ,  $h \in \mathbb{R}^N$ , and  $x \in \mathbb{R}^N$ . The equilibrium of this system

$$\mu = J^{-1}h$$

corresponds to the solution of the graph linear transformation introduced earlier. However, directly inverting J is computationally expensive and scales poorly with graph size.

# 2.2 Gaussian Belief Propagation

Instead of performing the matrix inversion, Gaussian Belief Propagation (GaBP) solves the system through localized message passing. In univariate GaBP, each message represents a univariate Gaussian distribution and is parameterized by two scalars: the precision  $\pi$  (inverse variance) and the information  $\eta$  (precision-weighted mean) [14, 16, 13]. At each iteration, node i sends a message to a neighbor

j based on incoming messages from all other neighbors except j, denoted  $\mathcal{N}(i) \setminus j$ . The message updates are defined as

$$\pi_{i \to j} = -\frac{J_{ij}^2}{\alpha_{i \setminus j}}, \qquad \eta_{i \to j} = -\frac{J_{ij}}{\alpha_{i \setminus j}} \, \beta_{i \setminus j},$$

where

$$\alpha_{i \setminus j} = J_{ii} + \sum_{k \in \mathcal{N}(i) \setminus j} \pi_{k \to i}, \qquad \beta_{i \setminus j} = h_i + \sum_{k \in \mathcal{N}(i) \setminus j} \eta_{k \to i}.$$

After convergence, the linear system  $J\mu=h$  is solved implicitly, and the resulting solution can be recovered by  $\mu_i=\eta_i/\pi_i$ .

**Convergence Guarantees.** GaBP is guaranteed to converge on cyclic graphs only when the precision matrix is walk-summable. Walk-summability requires that the normalized precision matrix  $\tilde{J} = D^{-1/2}JD^{-1/2}$  satisfy the spectral condition

$$\rho(|I - \tilde{J}|) < 1.$$

Under this condition, information propagation corresponds to a convergent geometric series,

$$\sum_{k=0}^{\infty} (I - \tilde{J})^k,$$

so that contributions from longer walks decay geometrically and the total influence of all walks remains finite.

# 3 Topologic Attention Networks

As discussed in the previous section, constructing an explicit graph linear transformation requires enumerating all paths between nodes, which is computationally intractable. Instead, we model information propagation as probabilistic inference over a walk-summable graph topology J. At equilibrium, GaBP satisfies

$$J\mu = h \quad \Rightarrow \quad \mu_i = \sum_j (J^{-1})_{ij} h_j,$$

where  $(J^{-1})_{ij}$  quantifies how information from node j influences node i through all paths in the graph. In this formulation, the effective neighborhood of a node can become dynamic in two senses. First, the precision matrix J determines which nodes are able to influence one another, so a node's neighborhood is defined by the topology encoded in J rather than by the raw graph adjacency. Second, the observation vector h determines how strongly the nodes within this topology contribute to the aggregation: nodes with weak evidence exert little influence, while

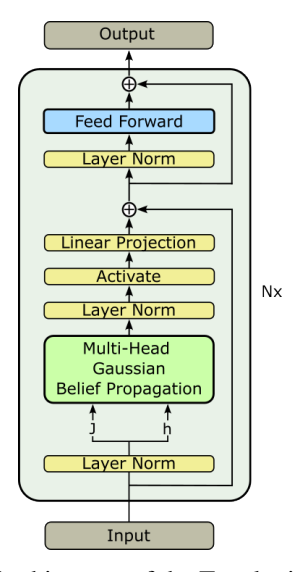


Figure 2: Architecture of the Topologic Attention Layer.

nodes with strong evidence have proportionally larger impact. Thus, J defines the dynamic neighborhood, and h defines the dynamic weighting within that neighborhood.

Building on this principle, we propose making the probabilistic inference learnable by parameterizing the node evidence h and, optionally, the topology J. This allows the model to jointly learn the topological neighborhoods and how strongly each node should participate in them. We refer to this as topologic attention, implemented through the Topologic Attention Layer.

#### 3.1 Topologic Attention Layer

The overall structure of the Topologic Attention Layer, illustrated in Figure 2, consists of two subblocks: a multi-head GaBP block followed by a node-wise feed-forward network. Each subblock applies layer normalization to the node features before processing, following the pre-normalization design shown to improve training stability in Transformer architectures [17]. In addition, the GaBP block applies a second layer normalization after the graph linear transformation to mitigate large, graph-dependent scale variations arising from the learned node degrees and edge weights. Since the GaBP operation itself is linear, a nonlinear activation function is applied to the updated node embeddings, which are then projected back to the original embedding dimension through a linear layer. Residual connections are incorporated around each subblock, prior to the normalization step.

#### 3.2 Modeling Assumptions

In GNNs, nodes are typically represented by multidimensional embeddings. Extending GaBP to be multivariate, where each node is multidimensional, causes the messages to be matrices that couple all embedding dimensions. To maintain scalability, we therefore make two simplifying assumptions. First, the neural network maps input features into an embedding space where dimensions can be treated as independent. Second, all dimensions share a single global precision matrix J. Intuitively, this means that each embedding dimension in h can be treated as its own univariate GaBP and is propagated through the same topology J.

## 3.3 Precision Matrix Designs

Different constructions of J induce distinct inductive biases and modes of topologic attention, helping to shape whether propagation behaves as local, global, smooth, or selective. We consider three walk-summable designs of J: Pairwise Normal, Diagonally Dominant, and Laplacian.

**Pairwise Normal** Pairwise-normalizable Gaussian graphical models span the same class of precision matrices as walk-summable models [13]. Each edge e=(i,j) contributes a local precision block

$$J^{(e)} = \begin{pmatrix} a_{ij} & b_{ij} \\ b_{ij} & c_{ij} \end{pmatrix}, \qquad a_{ij}c_{ij} > b_{ij}^2,$$

where the terms  $a_{ij}$  and  $c_{ij}$  represent the self-precisions of nodes i and j, while  $b_{ij}$  encodes their mutual coupling. For the full precision matrix J, each off-diagonal entry corresponds to the edge coupling  $J_{ij} = b_{ij}$ , and each diagonal entry aggregates a node's self-precision contributions from all adjacent edges:

$$J_{ii} = \sum_{j \in \mathcal{N}(i)} a_{ij}.$$

This construction induces a mutual-consistency bias, since the effective strength of an edge depends jointly on both endpoints: edges where either node has low self-precision contribute weak couplings, while edges supported by two confident nodes contribute strong ones. As a result, information propagation is naturally selective, emphasizing well-supported connections and attenuating uncertain or inconsistent ones.

**Diagonally Dominant** Diagonally dominant matrices are a subset of walk-summable matrices [14]. Such matrices are characterized by having each diagonal entry larger in magnitude than the sum of the magnitudes of the off-diagonal entries in the same row, that is,

$$J_{ii} > \sum_{j \neq i} |J_{ij}|.$$

In this design, each node is more confident in itself than in its connections to other nodes. This induces a confidence-centered bias, where information tends to flow outward from nodes with large diagonal precision and is absorbed more weakly by nodes with low self-precision. As a result, propagation becomes locally anchored, with high-confidence nodes acting as influential hubs and low-confidence nodes behaving primarily as receivers rather than broadcasters.

**Laplacian** Laplacian-based matrices are derived from the normalized graph Laplacian, defined as

$$L = I - D^{-\frac{1}{2}}AD^{-\frac{1}{2}},$$

where A is the weighted adjacency matrix and D is the corresponding degree matrix. The eigenvalues of L lie in the range (0,2); by rescaling them to (0,1), the resulting precision matrix is positive definite and walk-summable. In this design, information is smoothed according to the connectivity of the graph structure, inducing a manifold-smoothing bias where nodes embedded in similar structural environments co-vary strongly. As a result, propagation tends to operate at a community or cluster level, promoting broad diffusion over the graph while preserving contrasts between different structural regions.

#### 3.4 Learnable Components of Topologic Attention

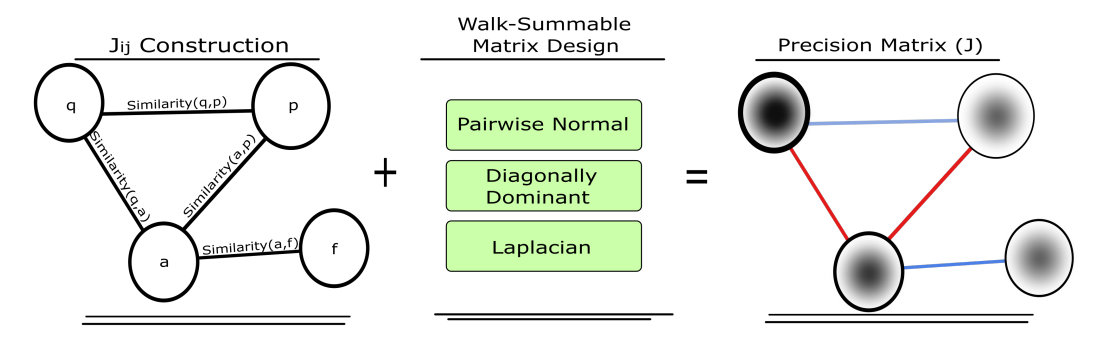


Figure 3: Depiction of how to construct a learned precision matrix J.

The observation vector h is obtained by projecting the node embeddings  $X \in \mathbb{R}^{N \times d_{\text{model}}}$  into a latent observation space via a trainable transformation:

$$h = \text{LeakyReLU}(XW_{\text{obs}}), \qquad W_{\text{obs}} \in \mathbb{R}^{d_{\text{model}} \times d_{\text{latent}}}.$$

When the precision matrix J is learned, its off-diagonal entries are derived from pairwise node similarities or reusing the observation vector. If new pairwise node similarities are used, they are computed from a learnable embedding

$$s = \text{LeakyReLU}(XW_{\text{sim}}), \quad W_{\text{sim}} \in \mathbb{R}^{d_{\text{model}} \times d_{\text{sim}}}.$$

For every edge (i, j), a scalar compatibility score is produced by a similarity function,

$$J_{ij} = \text{Similarity}(s_i, s_j),$$

implemented as an MLP, cosine similarity, or a Gaussian kernel. These raw scores serve as the initial edge strengths before being mapped into one of the walk-summable precision matrix constructions.

The choice of construction determines how the similarity-based edge strengths are converted into a valid precision matrix. For the learned Pairwise Normal model, cosine similarity provides the edge couplings  $b_{ij}$ , and nodewise self-precisions  $a_{ij}$  and  $c_{ij}$  are generated by neural mappings of the node embeddings and scaled to satisfy the constraint  $a_{ij}c_{ij} > b_{ij}^2$ . For the learned Diagonally Dominant model, cosine similarity parameterizes the off-diagonal terms  $J_{ij}$ , and the diagonal entries are formed by summing the magnitudes of the incident couplings. A learned nonnegative self-confidence term, obtained through a softplus transformation of the node embedding, allows each node to increase its own precision without strengthening its edges. For the learned Laplacian model, a Gaussian kernel on the similarity embeddings defines a weighted adjacency, which is degree-normalized and rescaled to ensure all eigenvalues lie strictly within (0,1). A small learnable diagonal contribution introduces slight node-specific variation while preserving the Laplacian structure. These mappings maintain the characteristic inductive biases of each construction while allowing the topology to adapt smoothly during training.

<sup>&</sup>lt;sup>1</sup>If the similarity function is not symmetric, we symmetrize the matrix as  $J = (J + J^{\top})/2$ .

#### 3.5 Multi-Head GaBP

The independence and parameter sharing assumptions, introduced for scalability, may be an oversimplification of the system dynamics that we want to model. To add expressiveness back into the model, we propose multi-headed GaBP, akin to multi-head attention in Transformers [18]. Through multi-headed GaBP, each head learns its own walk-summable topology  $J^{(k)}$  and observation vector  $h^{(k)}$ , and performs GaBP independently to obtain head-specific graph linear transformations. This formulation allows different heads to focus on distinct structural, semantic, or confidence contexts within the graph. The resulting node embeddings are layer-normalized, activated, concatenated, and projected back to the feature dimension.

## 3.6 Addressing the Unbounded Memory

Although Neural GaBP guarantees convergence under walk-summability, the number of iterations required to reach convergence is unknown. This poses a challenge for training, as it would require storing an unknown number of iteration messages for each layer. To address this, we adopt an implicit differentiation strategy that computes exact gradients at convergence without unrolling the iterative inference process. At convergence, the solution satisfies  $J\mu=h$ . Differentiating with respect to the model parameters  $\theta$  gives the corresponding forward and backward relations:

$$J\frac{d\mu}{d\theta} + \frac{dJ}{d\theta}\mu = \frac{dh}{d\theta} \Rightarrow J\frac{d\mathcal{L}}{dh} = \frac{d\mathcal{L}}{d\mu}.$$

This relation allows gradients to be computed directly at the fixed point using the same GaBP solver as in the forward pass, eliminating the need to store intermediate messages. This reduces memory complexity from O(TE) to O(E+N), trading additional compute for substantial memory savings.

# 4 Experimental Setup

We evaluate the performance of learned and fixed topologies for TANs across six benchmark datasets with cyclic graph structures under both homogeneous and heterogeneous learning settings. The Cora, Citeseer, and PubMed citation datasets serve as representative homogeneous benchmarks, while the Texas, Wisconsin, and Cornell datasets serve as representative heterogeneous benchmarks. These six datasets each represent a single, static graph and are used for transductive node classification.

We compare our method against foundational and representative models from the other two branches of dynamic neighborhood aggregation, along with standard local aggregation methods. Specifically, we include the Graph Convolutional Network (GCN) and Graph Attention Network (GAT) as representative local aggregation models. For methods that perform global or continuous neighborhood aggregation, we evaluate against the Structure-Aware Transformer (SAT) [19], an adapted Graphormer designed for node classification rather than graph classification, as well as the Graph Neural Differential Equation (GDE) and Continuous Graph Neural Network (CGNN).

To ensure a fair comparison across all models, we use a consistent architecture with the hidden dimensions fixed at 64. Each method is implemented with two layers of its respective aggregation mechanism. For attention-based architectures, each layer employs eight attention heads in the first layer and a single head in the second layer. Each first layer head outputs eight features, while the second layer head outputs all 64 features. This setup controls for model capacity so the differences primarily reflect the behavior of each aggregation mechanism rather than variations in network depth or parameter count.

All models are trained using the Adam optimizer with weight decay  $5 \cdot 10^{-4}$ , early stopping with a patience of 100 epochs and a dropout of 0.6, except the fixed Laplacian which used a patience of 200 epochs. The learning rate for the TAN and SAT models are  $1 \cdot 10^{-3}$  while the learning rate for the other models are  $1 \cdot 10^{-2}$ . The tolerance for the GaBP in the Topologic Attention Layers is set to  $1 \cdot 10^{-6}$  and a maximum iteration count was set to 1000. To ensure stable convergence on graphs with loops, we apply message damping with a coefficient of  $\lambda = 0.5$ .

For each dataset, we adopt random node splits preserving the original train/validation/test ratios but do not enforce class balance. This setup better reflects realistic scenarios where labeled nodes are unevenly distributed across classes, providing a more robust measure of generalization [20]. Each

experiment is repeated across 30 random runs, each with independently sampled splits. We report the mean  $\pm$  standard deviation of test accuracy.

For TAN, we ensure the graph is undirected and self loops are removed since the diagonal entries of the precision matrix J already encode each node's self-precision. For the other models, we ensure self loops.

#### 5 Results

Table 1 reports the performance across all benchmark datasets. Overall, TAN achieves improved generalization on all measured baselines. Within TAN, we implemented six variants: a learnable and

Table 1: The test accuracy in % evaluation datasets. **Bold** numbers indicate the best performance, while <u>underline</u> indicate second best performance. "OOM" denotes out-of-memory errors encountered during training. (L) denotes a learned precision matrix while (F) denotes a fixed precision matrix.

Homophily	Texas 0.11	Wisconsin 0.21	Cornell 0.30	Cora 0.81	Citeseer 0.74	Pubmed 0.80
GCN	60.6±5.3	61.0±0.6	62.5±0.9	80.2±0.3	65.3±0.6	75.6±0.3
GAT	$48.6\pm0.1$	$64.5 \pm 2.5$	$63.4\pm5.5$	$76.6\pm1.1$	$\frac{63.5\pm0.0}{64.6\pm1.8}$	$\frac{73.0\pm0.5}{74.0\pm0.5}$
SAT	$77.8\pm2.6$	$82.7\pm2.4$	$77.9\pm2.6$	$53.5 \pm 1.4$	$47.6 \pm 1.0$	OOM
Graphormer	$69.4 \pm 7.6$	$\frac{62.7\pm2.4}{65.2\pm4.3}$	57.7±2.0	31.7 + 2.3	28.7 + 3.4	OOM
GDE	$57.8\pm6.2$	$55.9 \pm 1.6$	$60.0 \pm 2.9$	$80.1 \pm 1.3$	$65.1 \pm 1.6$	$75.0\pm0.9$
CGNN	$52.3\pm1.7$	$75.2\pm1.8$	$66.8 \pm 1.2$	$73.9 \pm 0.2$	$65.2 \pm 0.5$	$74.9\pm0.4$
Ours						
(L) Pairwise Normal	$82.1 \pm 4.2$	$78.1 \pm 2.2$	$75.5 \pm 4.3$	$46.4 \pm 1.2$	$39.0 \pm 1.2$	$64.1 \pm 1.3$
(L) Diagonally Dominant	$83.7 \pm 3.7$	$76.5 \pm 1.8$	$74.9 \pm 4.6$	$47.7 \pm 1.3$	$41.9 \pm 1.5$	$62.3 \pm 1.5$
(L) Laplacian	$61.1 \pm 7.3$	$76.1 \pm 3.1$	$63.7 \pm 3.9$	$80.4 \pm 1.3$	$64.5 \pm 1.3$	$74.2 \pm 1.4$
(F) Pairwise Normal	$82.7 \pm 3.4$	$76.8 \pm 1.9$	$80.2 \pm 4.0$	$44.8 \pm 1.0$	$39.4 \pm 1.4$	$66.0 \pm 1.7$
(F) Diagonally Dominant	$\overline{56.2 \pm 7.0}$	$68.4 \pm 3.0$	$\overline{57.0\pm5.2}$	$80.6 {\pm} 1.2$	$65.1 \pm 1.4$	$75.3 \pm 0.9$
(F) Laplacian	$77.8 \pm 10.3$	$83.1 {\pm} 2.0$	$81.3 \pm 2.3$	$71.9 \pm 1.4$	$66.0 {\pm} 1.8$	$76.8 \pm 1.0$

a fixed versions of each precision matrix. The fixed Laplacian construction, although walk-summable, was the only variant that did not converge within the maximum iterations. This occurs because normalized Laplacian topologies place much of their spectrum very close to the walk-summability boundary, which results in extremely slow GaBP contraction even after symmetric normalization and scaling. As a result, both the forward graph linear transformation and the backward implicit-differentiation were computed using partially converged solutions. This produced noisy graph linear transformations and gradients which made early training difficult; however once the model began to form stable representations, the fixed Laplacian variant was the most general matrix construction tested with state-of-the-art accuracy in five out of six datasets. This suggests that exact GaBP convergence is not always necessary for effective learning.

For the other matrix constructions, the learned precision matrices always converged under the GaBP solver, requiring no more than 100 iterations to reach the tolerance threshold. The fixed Diagonally Dominant and fixed Pairwise Normal constructions also converged consistently, although they typically required more iterations than their learned counterparts, reaching at most about 150 iterations.

# 6 Conclusion

This work introduced TANs, which implement topologic attention by learning how information should flow probabilistically through the graph's topology. TANs achieve this by using Gaussian Belief Propagation to exchange messages between nodes, allowing each node to integrate both direct and indirect influences. Across both homophilic and heterophilic benchmarks, TANs consistently surpassed the measured baselines.

A particularly notable finding was that the fixed Laplacian variant achieved high accuracy even when GaBP did not fully converge. This result suggests that partially converged GaBP solutions may

introduce useful inductive biases or implicit regularization effects. Further investigation into these approximate solutions may reveal new opportunities for designing efficient inference procedures that maintain strong generalization performance.

We are excited to see the future development of TANs. One important challenge for wider adoption is improving the efficiency of GaBP on arbitrary graphs. Because GaBP is an iterative algorithm, incorporating multigrid techniques [21] or other hierarchical solvers may lead to significantly faster convergence and better scalability, which would enable TANs to operate effectively on large or streaming graph datasets.

#### References

- [1] Thomas N. Kipf and Max Welling. Semi-supervised classification with graph convolutional networks. In *International Conference on Learning Representations (ICLR)*, 2017. URL https://arxiv.org/abs/1609.02907. arXiv preprint arXiv:1609.02907.
- [2] Petar Veličković, Guillem Cucurull, Adriana Casanova, Adriana Romero, Pietro Liò, and Yoshua Bengio. Graph attention networks. *arXiv preprint arXiv:1710.10903*, 2017.
- [3] Vijay Prakash Dwivedi, Ladislav Rampăšek, Mikhail Galkin, Amir Parviz, Guy Wolf, Anh Tuan Luu, and Dominique Beaini. Long range graph benchmark (lrgb). In *Proceedings of the 36th Conference on Neural Information Processing Systems (NeurIPS 2022), Datasets and Benchmarks Track*, 2022. URL https://papers.neurips.cc/paper\_files/paper/2022/file/8c3c666820ea055a77726d66fc7d447f-Paper-Datasets\_and\_Benchmarks.pdf.
- [4] Dong Chen, Thomas H. Schulz, and Karsten Borgwardt. Learning long range dependencies on graphs via random walks. In *Proceedings of the International Conference on Learning Representations (ICLR 2025)*, 2025. URL https://proceedings.iclr.cc/paper\_files/paper/2025/file/f039f5b34b2c2ae27808cf2a01ac3306-Paper-Conference.pdf.
- [5] Michael Poli, Stefano Massaroli, Junyoung Park, Atsushi Yamashita, Hajime Asama, and Jinkyoo Park. Graph neural ordinary differential equations. *arXiv preprint arXiv:1911.07532*, 2019. URL https://arxiv.org/abs/1911.07532.
- [6] Louis-Pascal A. C. Xhonneux, Meng Qu, and Jian Tang. Continuous graph neural networks. *arXiv preprint arXiv:1912.00967*, 2019. URL https://arxiv.org/abs/1912.00967.
- [7] Nan Yin, Mengzhu Wang, Li Shen, Hitesh Laxmichand Patel, Baopu Li, Bin Gu, and Huan Xiong. Continuous spiking graph neural networks (cos-gnn). *arXiv preprint arXiv:2404.01897*, 2025. Version v2, submitted July 12 2025.
- [8] Vijay Prakash Dwivedi and Xavier Bresson. A generalization of transformer networks to graphs. *arXiv preprint arXiv:2012.09699*, 2020. URL https://arxiv.org/abs/2012.09699.
- [9] Chengxuan Ying, Tianle Cai, Shengjie Luo, Shuxin Zheng, Guolin Ke, Di He, Yanming Shen, and Tie-Yan Liu. Do transformers really perform bad for graph representation? *arXiv* preprint *arXiv*:2106.05234, 2021. URL https://arxiv.org/abs/2106.05234.
- [10] Yinan Huang, William Lu, Joshua Robinson, Yu Yang, Muhan Zhang, Stefanie Jegelka, and Pan Li. On the stability of expressive positional encodings for graphs. In *International Conference on Learning Representations (ICLR)*, 2024. URL https://openreview.net/pdf?id=xAqcJ9XoTf.
- [11] Karsten M. Borgwardt and Hans-Peter Kriegel. Shortest-path kernels on graphs. In *Proceedings* of the 5th IEEE International Conference on Data Mining (ICDM '05), page 74–81, Houston, TX, USA, 2005. IEEE Computer Society.
- [12] Thomas Gärtner, Peter A. Flach, and Stefan Wrobel. On graph kernels: Hardness results and efficient alternatives. In *Proceedings of the 16th Annual Conference on Computational Learning Theory (COLT) / 7th Kernel Workshop*, volume 2777 of *Lecture Notes in Computer Science*, pages 129–143. Springer, 2003. doi: 10.1007/978-3-540-45167-9\\_11.

- [13] Dmitry Malioutov, Jason K. Johnson, and Alan S. Willsky. Walk-sums and belief propagation in gaussian graphical models. Journal of Machine Learning Research, 7:2031–2064, 2006.
- [14] Danny Bickson. Gaussian Belief Propagation: Theory and Application. PhD thesis, The Hebrew University of Jerusalem, 2008. URL https://www.cs.huji.ac.il/~dolev/pubs/ thesis/phd-thesis-bickson.pdf.
- [15] Joseph Ortiz, Talfan Evans, and Andrew J. Davison. A visual introduction to gaussian belief propagation. arXiv preprint arXiv:2107.02308, 2021.
- [16] Jason K. Johnson, Danny Bickson, and Danny Dolev. Fixing convergence of gaussian belief propagation. arXiv preprint arXiv:0901.4192, 2009. URL https://arxiv.org/abs/0901. 4192.
- [17] Ruibin Xiong, Yunchang Yang, Di He, Kai Zheng, Shuxin Zheng, Chen Xing, Huishuai Zhang, Yanyan Lan, Liwei Wang, and Tie-Yan Liu. On layer normalization in the transformer architecture. In Proceedings of the 37th International Conference on Machine Learning (ICML 2020), page 10524–10534, 2020.
- [18] Ashish Vaswani, Noam Shazeer, Niki Parmar, Jakob Uszkoreit, Llion Jones, Aidan N. Gomez, Łukasz Kaiser, and Illia Polosukhin. Attention is all you need. In Advances in Neural Information Processing Systems (NeurIPS), pages 5998–6008, 2017. https://arxiv.org/abs/ 1706.03762.
- [19] Dexiong Chen, Leslie O'Bray, and Karsten Borgwardt. Structure-aware transformer for graph representation learning. arXiv preprint arXiv:2202.03036, 2022. URL https://arxiv.org/ abs/2202.03036.
- [20] Oleksandr Shchur, Maximilian Mumme, Aleksandar Bojchevski, and Stephan Günnemann. Pitfalls of graph neural network evaluation. arXiv preprint arXiv:1811.05868, 2019.
- [21] William Briggs, Van Henson, and Steve McCormick. A Multigrid Tutorial, 2nd Edition. 01 2000. ISBN 978-0-89871-462-3.

# **Appendix**

#### A.1 Psuedocode for Gaussian Belief Propagation

We provide the psuedocode for GaBP as a convenient understanding for the math presented in the background section.

#### **Algorithm 1** Gaussian Belief Propagation

- 1: **Input:**  $J, h, \varepsilon, \lambda$
- 2: Initialize  $\pi_{i \to j} = 0$ ,  $\eta_{i \to j} = 0$
- 3: **while** not converged  $(\Delta > \varepsilon)$  **do**
- $\alpha_{i \setminus j} = J_{ii} + \sum_{k \in N(i) \setminus j} \pi_{k \to i}$  $\beta_{i \setminus j} = h_i + \sum_{k \in N(i) \setminus j} \eta_{k \to i}$

- $\pi_{i \to j}^{\text{new}} = -J_{ij}^2/\alpha_{i \setminus j}$   $\eta_{i \to j}^{\text{new}} = -J_{ij}\beta_{i \setminus j}/\alpha_{i \setminus j}$
- $\pi_{i \to j} \leftarrow (1 \lambda) \, \pi_{i \to j} + \lambda \, \pi_{i \to j}^{\text{new}}$
- $\eta_{i \to j} \leftarrow (1 \lambda) \, \eta_{i \to j} + \lambda \, \eta_{i \to j}^{\text{new}}$
- $\Delta = \max_{(i,j)}(|\Delta \pi_{i \to j}|, |\Delta \eta_{i \to j}|)$
- 11: end while
- 12: **Output:**  $\mu_i = \eta_i / \pi_i$

## A.2 Evolution of GaBP Iterations During Training

Since TANs rely on GaBP to perform the graph linear transformation at each layer. We wanted to analyze how the number of GaBP iterations evolves over the course of training for the learned precision matrices. We visualize (Figures the convergence behavior along with the accuracy on Wisconsin dataset the three learned precision matrices. We chose the Wisconsin dataset to analyze because the learned matrices achieved similar accuracy on the dataset. We ran the models for 500 epochs. We also visualize the diagonally dominant matrix for the Pubmed dataset. Interestingly, across the analyzed datasets, the iterations decrease as training progresses. Moreover, the dataset does not appear to overfit to the dataset.

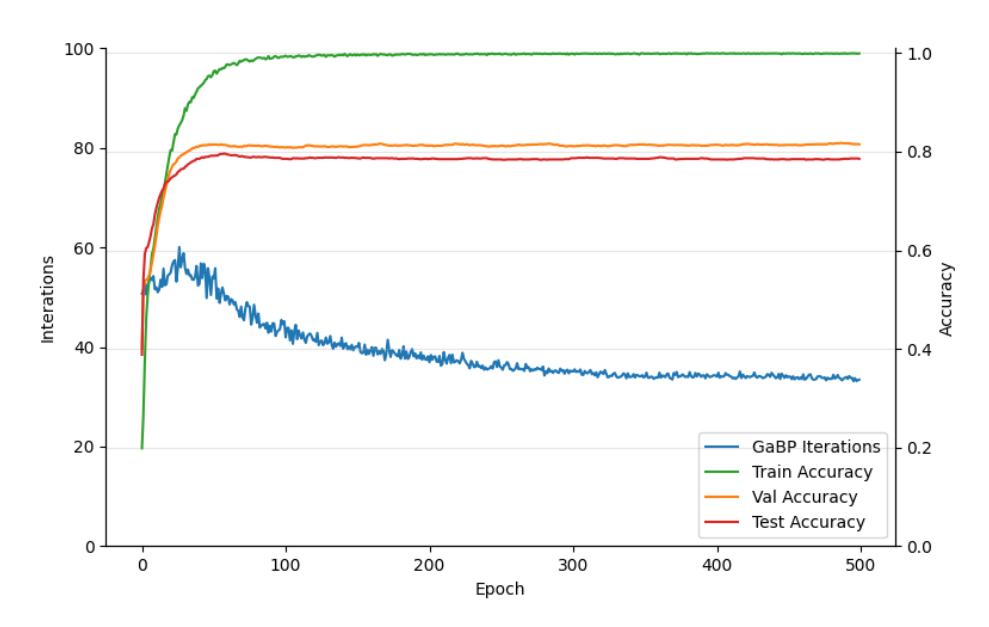


Figure 4: Training Over Time of the Diagonally Dominant Precision Matrix on the Wisconsin Dataset.

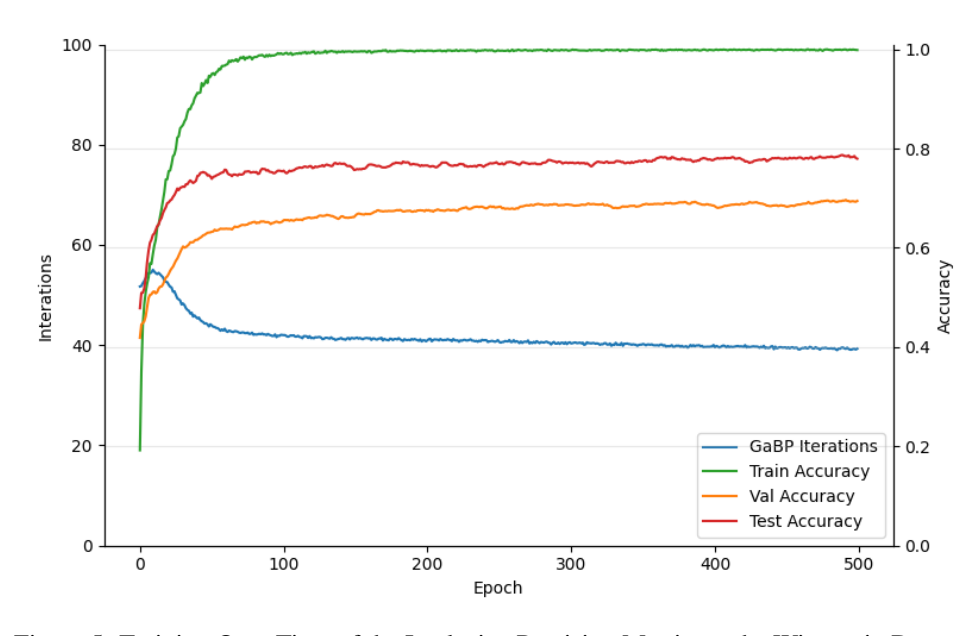


Figure 5: Training Over Time of the Laplacian Precision Matrix on the Wisconsin Dataset.

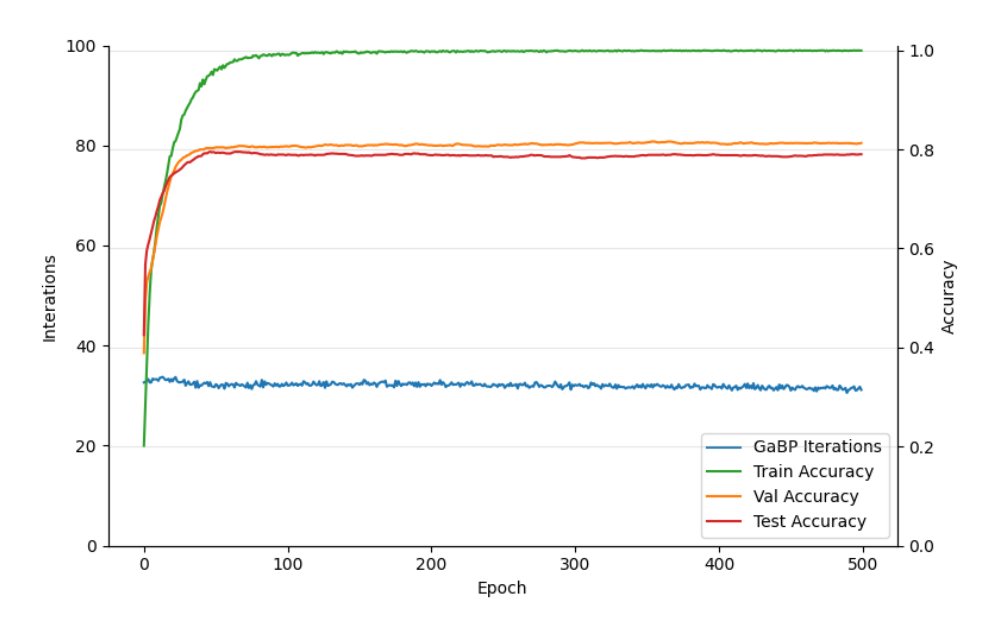


Figure 6: Training Over Time of the Pairwise Normal Matrix on the Wisconsin Dataset.

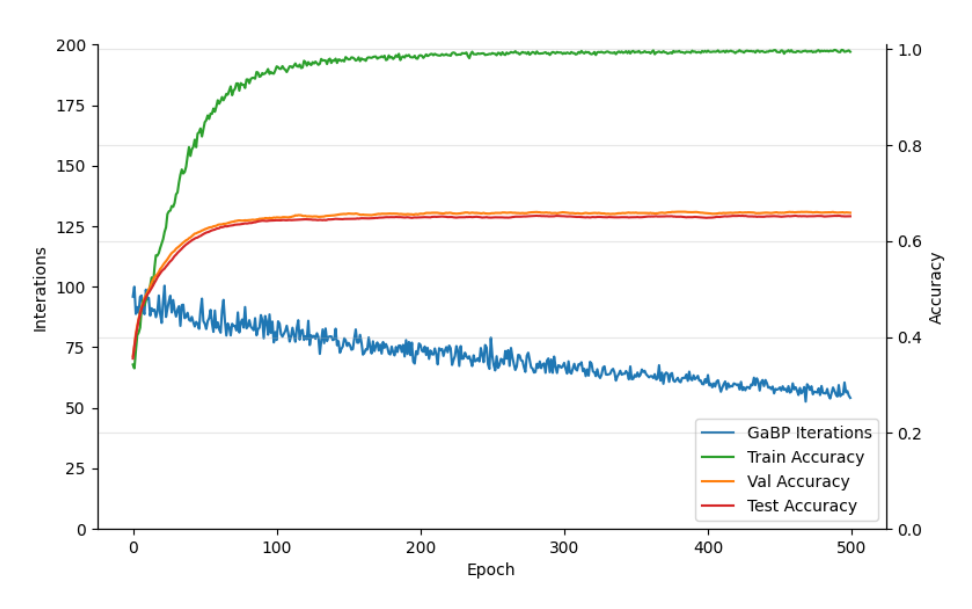


Figure 7: Training Over Time of the Diagonally Dominant Precision Matrix on the Pubmed Dataset.

# A.3 Analysis of the Biases of Matrix Constructions

To understand how each precision matrix construction shapes the topology, we visualize the correlation matrix (Figures 8–11) on the Wisconsin dataset. For the learned precision matrices, we visualize the first-layer. These correlation matrices are computed from the inverse precision matrix and describe how strongly two nodes would co-vary under the learned topology in the absence of any observation vector h. They therefore characterize the influence structure implied by J, meaning the potential pathways and relative strengths along which GaBP is capable of transmitting information, regardless of the actual evidence supplied during inference. Red values indicate positive correlations and blue values indicate negative correlations, with intensity proportional to magnitude. Nodes are ordered by the second eigenvector to highlight community structure, and the accompanying adjacency

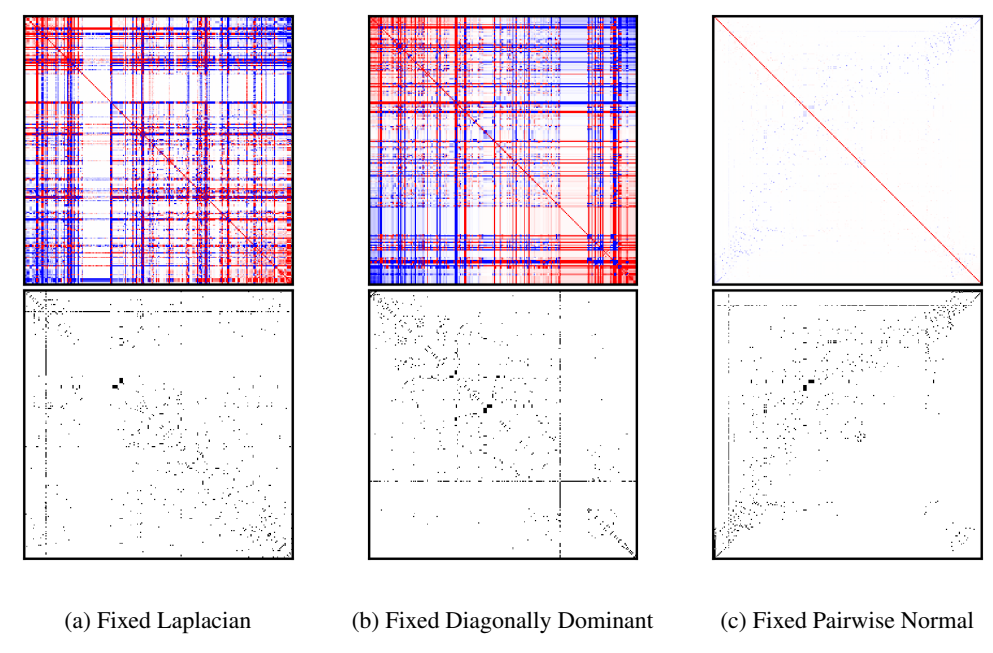


Figure 8: Comparison of fixed precision matrix constructions on the Wisconsin dataset.

matrices (bottom panels), ordered in the same way, show the corresponding learned connectivity patterns.

**Learned Laplacian Construction.** The Laplacian-based precision matrix produces a pronounced block structure resembling a plaid pattern of alternating positive and negative correlations. Nodes form compact clusters with internal correlations, while inter-cluster relationships often alternate in sign, indicating that the model captures both homophilic and heterophilic dependencies. The dense regions along the diagonal of the reordered adjacency matrix confirm the emergence of localized communities. Because the Laplacian construction constrains the eigenvalues of the precision matrix to lie within (0,1), each node contributes with comparable influence to the overall propagation. Most of the learning therefore occurs through topologic deformation, where the model folds the underlying space before blending node representations. As a result, this design behaves like a band-pass filter in the topologic attention, supporting community-level diffusion over a learned relational manifold while maintaining structured contrast between clusters.

Learned Diagonally Dominant Construction. In the diagonally dominant formulation, a few high-confidence nodes can exert strong influence over their neighborhoods. Because each node's self-term dominates its row in J, information primarily flows outward from confident nodes rather than through collective averaging. Each node is equipped with a learned confidence gate that dynamically adjusts its self-precision, regulating how much information it absorbs from its neighbors. As a result, highly confident nodes act as local leaders within the topologic attention, shaping how propagation unfolds across the graph. When node confidences are comparable, correlations weaken, leading to sparse yet focused connectivity patterns or minimal inter-node correlation. The more uniform edge spread observed in the adjacency view reflects this shift from community-level organization toward node-level importance. Overall, this design behaves as a low-pass filter centered around the most confident nodes.

**Learned Pairwise Normal Construction.** The pairwise normal matrix yields the most selective propagation pattern. Since each edge's contribution depends on the mutual confidence of its connected nodes, information flows only where representations are jointly compatible. This formulation models each edge as the agreement both endpoints have in their connection, scaling similarity by their confidence ratio and emphasizing edges supported by reciprocal certainty. Consequently, propagation strength is highest along confident paths and suppressed in uncertain regions, requiring mutual trust

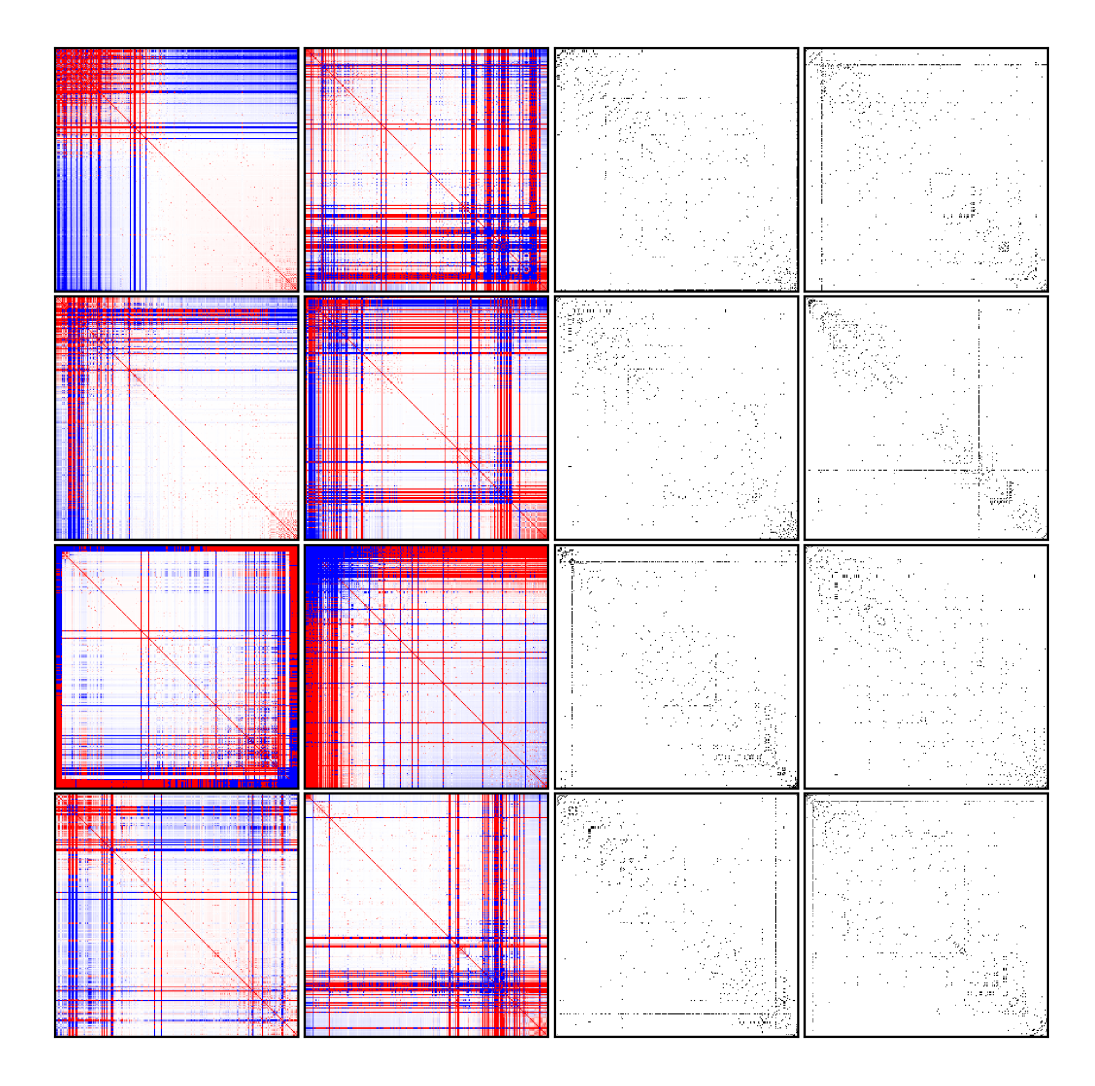


Figure 9: Learned Laplacian precision construction. The Laplacian matrix induces community-level smoothness and alternating cluster correlations.

for effective global communication. The resulting correlations form gradual gradients rather than sharp blocks, functioning as a high-pass filter in low-correlation areas and a low-pass filter in highly correlated areas. The corresponding adjacency maps reveal clearer separation between sparse and dense zones, indicating that low-degree nodes propagate information more readily than high-degree ones, where competition among edges dampens transmission. Overall, this design emphasizes strong, well-supported relationships while attenuating weak or inconsistent ones, producing structured selectivity in topologic attention.

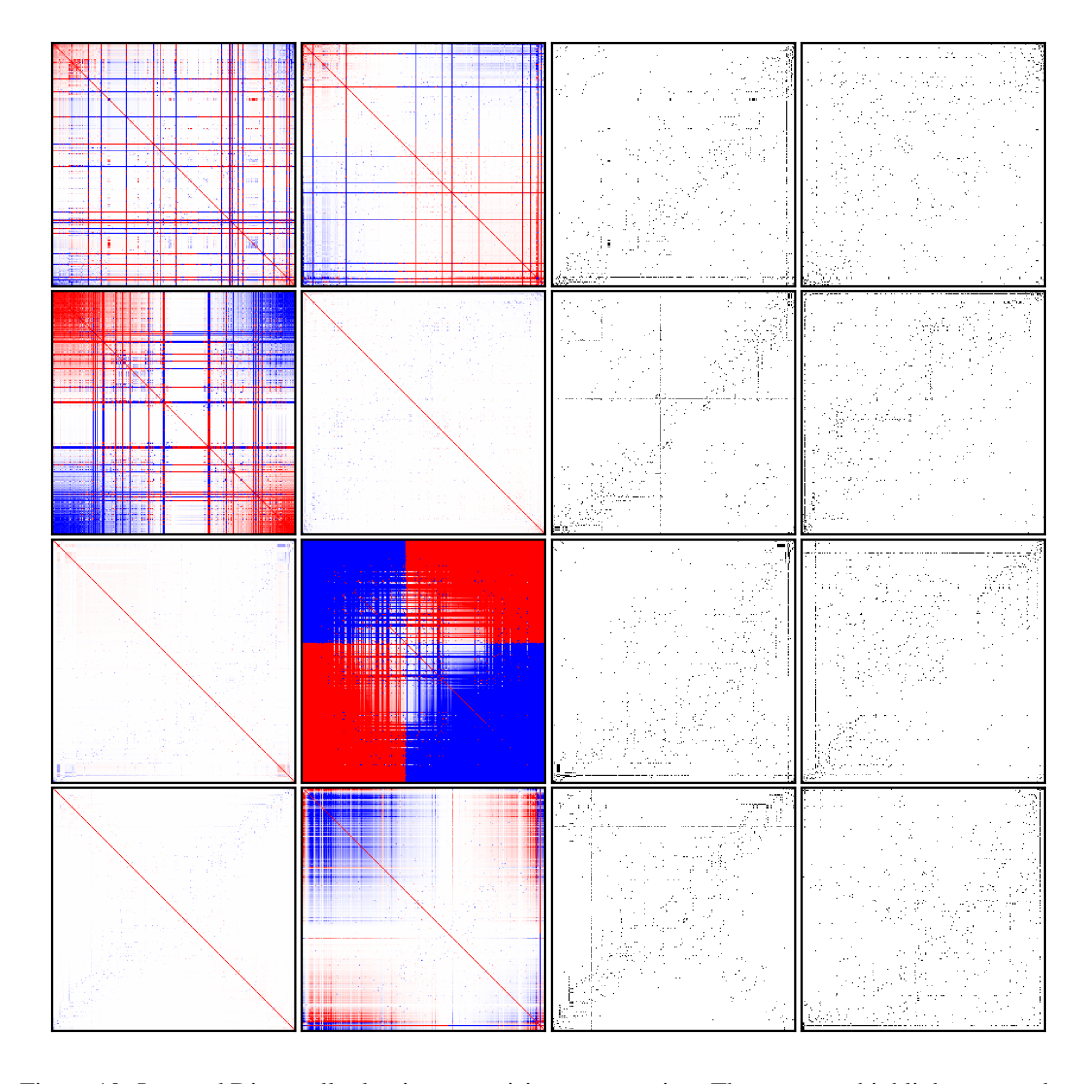


Figure 10: Learned Diagonally dominant precision construction. The structure highlights sparse but concentrated correlations driven by high-confidence nodes.

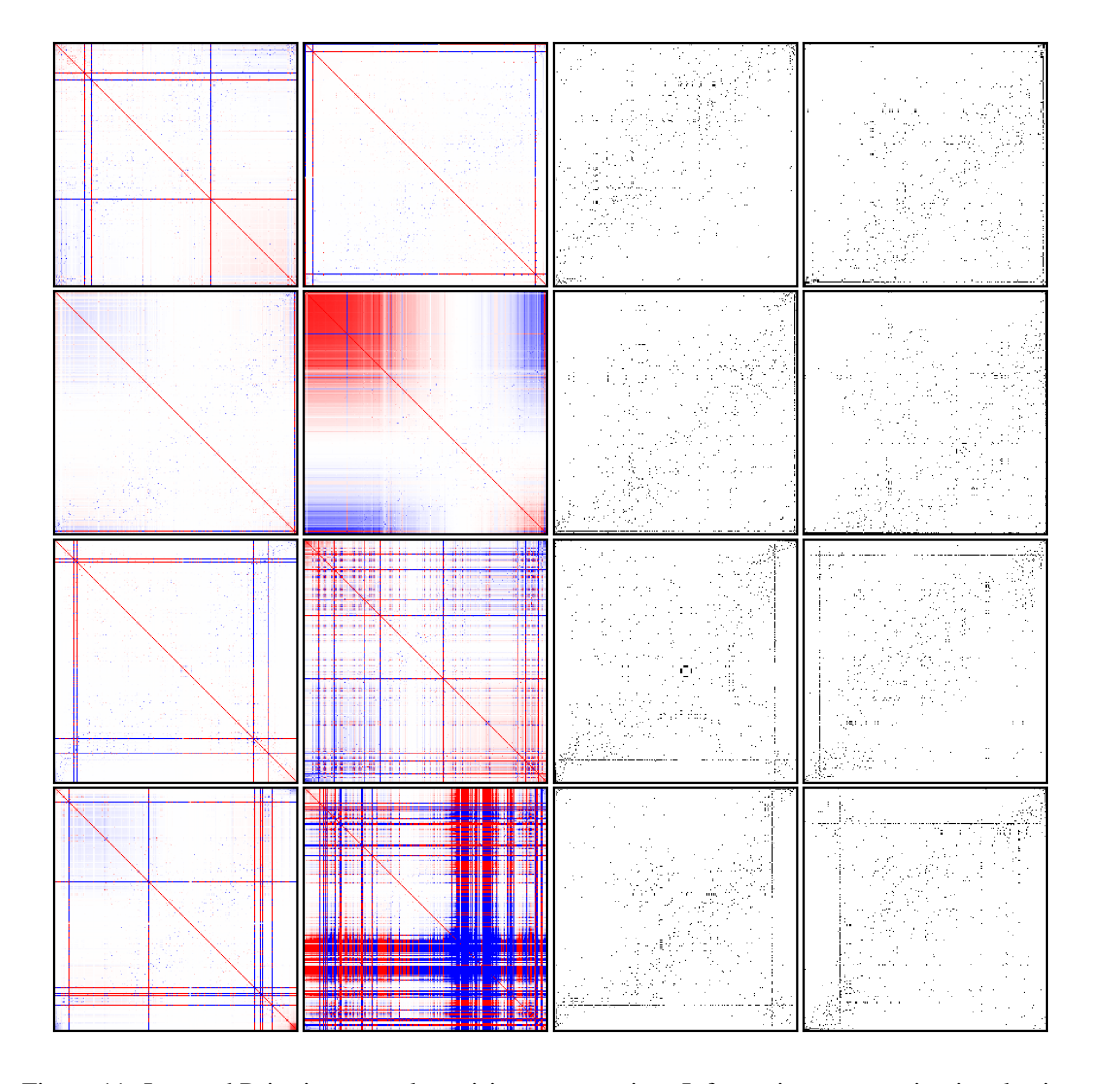


Figure 11: Learned Pairwise normal precision construction. Information propagation is selective, reflecting mutual agreement between connected nodes.